Available online at www.sciencedirect.com
SCIENCE DIRECT
Vibrational Spectroscopy 40 (2006) 168–176
VIBRATIONAL SPECTROSCOPY
www.elsevier.com/locate/vibspec

Absolute integrated infrared intensities of liquid fluorobenzene between 4000 and 400 cm^{-1} at 25 °C

C. Dale Keefe *, Jennifer L. MacDonald

Department of Physical and Applied Sciences, Cape Breton University, 1250 Grand Lake Road, Sydney, NS, Canada B1P 6L2

Received 27 June 2005; received in revised form 17 August 2005; accepted 22 August 2005
Available online 6 October 2005

Abstract

This paper is a continuation of the study of the integrated absorption intensities of benzene and its simple derivatives. In this paper, the imaginary molar polarizability spectrum reported earlier for fluorobenzene was fit with 169 classical damped harmonic oscillator bands. The standard deviation and RMSE of the fit are both 0.006 cm^3 $mol^{-1}$and the area under the fitted spectrum is 0.5% larger than the area under the experimental spectrum. Most of the required peaks are assigned to fundamentals, first overtones or binary combinations. From the parameters of the fitted peaks, the integrated intensities, transition moments and dipole moment derivatives with respect to normal coordinates of the infrared active fundamentals are determined. The F-Sum rule is used to compare the integrated intensities to those of benzene and bromobenzene in the literature. Remarkably, the F-Sums of the out-of-plane vibrations are the same in all the molecules while the in-plane F-Sums vary markedly between the different molecules.

Keywords: Fluorobenzene; Integrated infrared intensities; Dipole moment derivatives; Transition moments; Liquid; Curvefit; Polarizability

1. Introduction

Over the last decade, this laboratory has been involved in the exploration of the absolute infrared vibrational intensities of benzene and benzene derivatives in the liquid phase. The focus of this project is to understand how the intermolecular interactions in the liquid affect the vibrational intensities. Interest in the vibrational properties of benzene dates back to the 1930s with the work of Wilson [1].

The integrated intensities in the liquid phase are obtained from the imaginary molar polarizability spectrum, which is determined from the complex refractive index spectra across the infrared. For a review of how one obtains complex refractive index spectra and the conversion to the imaginary molar polarizability spectrum, the reader is referred to Ref. [2] and references cited therein. Once the imaginary molar polarizability spectrum is known, the integrated intensities of the various transitions need to be determined. This is done by fitting the imaginary molar polarizability spectrum to a standard lineshape. The preferred [2–4] lineshape for the imaginary molar polarizability spectrum is the classical damped harmonic oscillator (CDHO) lineshape. From the integrated intensities, the transition moments and dipole moment derivatives can be obtained. It is these quantities that are compared between the different benzene compounds to gain insight into how the liquid phase vibrational intensities are dependent on the intermolecular interactions.

To date, the complex refractive index spectra, imaginary molar polarizability spectra, transition moments and dipole moment derivatives have been reported for benzene [5–7], benzene-d_6 [8], benzene-d_1 [9], bromobenzene [10,11], bromobenzene-d_5 [12,13] and hexafluorobenzene [14,15]. In addition, the complex refractive index spectra and imaginary molar polarizability spectra of ethylbenzene [16], fluorobenzene [17], toluene [18], and toluene-d_8 [19] have been reported. In this paper, the fit and integrated intensities of fluorobenzene are reported. Work is presently underway in this laboratory to fit the imaginary molar polarizability spectra of the remainder of these compounds.

In addition, the experimental intensities and force field of three isotopomers of liquid benzene (-h_6, -d_6, -d_1) have been used to compare the dipole moment derivatives with respect to symmetry and internal coordinates [20]. These dipole moment derivatives were also compared to the corresponding experimental derivatives of gaseous benzene [21]. It was found that while the experi-

* Corresponding author. Tel.: +1 902 563 1185; fax: +1 902 563 1880.
E-mail address: dale_keefe@capebretonu.ca (C.D. Keefe).

0924-2031/$ – see front matter © 2005 Elsevier B.V. All rights reserved.
doi:10.1016/j.vibspec.2005.08.003

mental intensities are different for the three isotopomers in the liquid and gas phase, these differences are due essentially to a difference in the CH stretch dipole moment derivative. This difference was related qualitatively to the intermolecular interaction of the H with the π-cloud of the nearest neighbour creating a pseudo-hydrogen bond. The dipole moment derivatives of the gas were also recently [22] calculated via ab initio calculations using various levels of theory and basis sets.

This paper reports the fitting of the optical constants (real and imaginary refractive indices) and imaginary polarizability spectrum, α''_m, calculated under the Lorentz local field of fluorobenzene reported previously [17] between 4000 and 400 cm^{-1}. Most of the required peaks were due to observable features within the spectrum. The assignments of most of the features in the infrared spectrum of liquid fluorobenzene are reported. The integrated intensities and transition moments are compared to those of several benzene derivatives.

2. Experimental

2.1. Fitting the imaginary molar polarizability spectrum

By using the curvefitting program SPECFIT [23], the imaginary molar polarizability spectrum from 4000 to 400 cm^{-1} was fitted using CDHO bands. The fitting process began by splitting the full spectrum into smaller regions and fitting each separately. This allowed for changes in the fitted spectrum to be adjusted more quickly. The full spectrum was then fitted, refining the peaks from the separate regions. This fit required 169 peaks. The standard deviation of the fit is 0.006 $cm^3\ mol^{-1}$, the root-mean-square error is 0.006 $cm^3\ mol^{-1}$, and the multiple coefficient of determination [24], R^2 is 0.99983, indicating a very good fit. The total area under the fitted spectrum between 3950 and 400 cm^{-1} is 0.5% larger than the corresponding area under the experimental spectrum.

SPECFIT outputs the peak wavenumber, $\tilde{\nu}_j$; the full width at half height (FWHH), Γ_j; and a constant, Y_j, that is the peak height of the corresponding band in the $\tilde{\nu}\alpha''_m$ spectrum multiplied by the FWHH. The complete integrated intensity under the α''_m band, C_j, can be obtained from Y_j through $C_j = Y_j\pi/2$. The parameters $\tilde{\nu}_j$, Γ_j, and C_j of the fitted bands are given in Table 1, as well as the observed positions of the features of the experimental spectrum. Several of the observed features were ignored in the fit. These generally are assigned to water vapour or features next to much stronger ones where the uncertainties in fitting the stronger features were larger than the weaker features making any attempt to fit them meaningless.

The quality of the fit is shown in Fig. 1. On the actual scale, the experimental and fitted spectra are superimposed. On the expanded scale, differences are visible at ∼3400, ∼3200, ∼3000, and ∼2800 cm^{-1} in the top box. In the middle

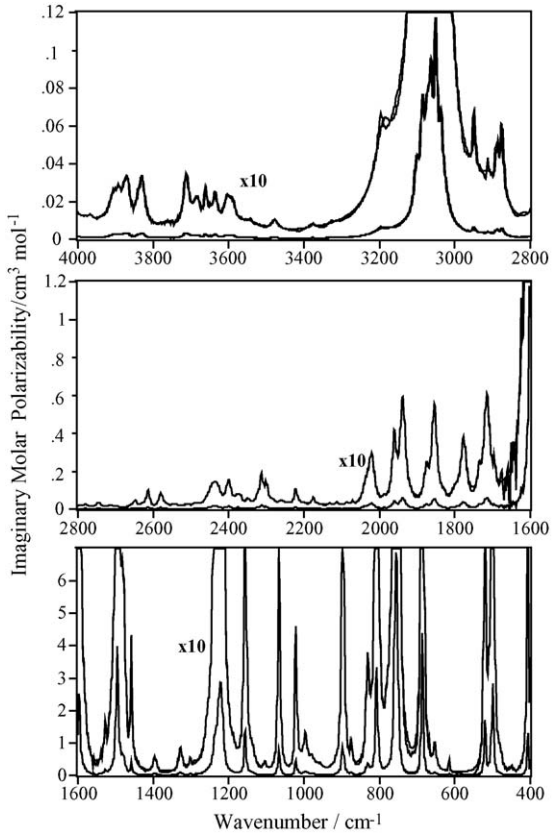

Fig. 1. The experimental and fitted imaginary molar polarizability spectra of liquid fluorobenzene at 25 °C between 4000 and 400 cm^{-1}. The upper spectra in each box are the experimental and fitted spectra multiplied by 10.

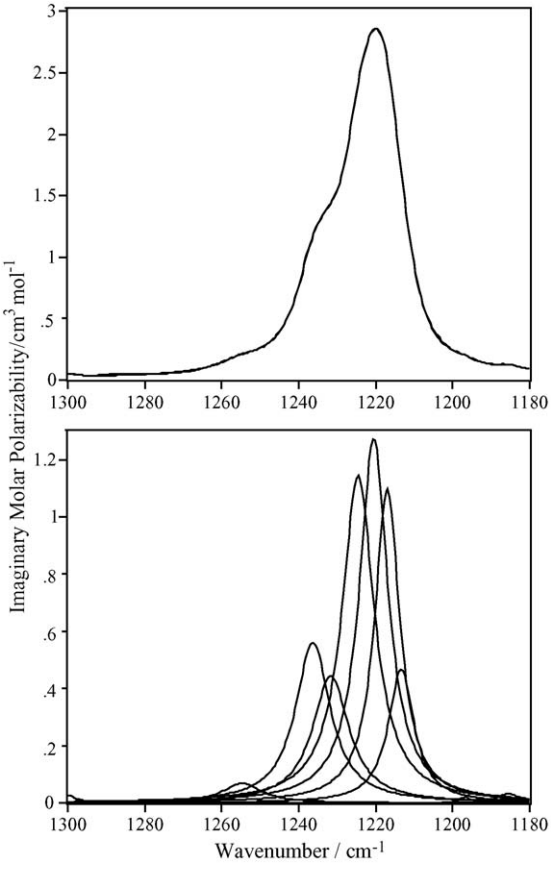

Fig. 2. The experimental and fitted imaginary molar polarizability spectra (top box) of liquid fluorobenzene at 25 °C between 1300 and 1180 cm^{-1} and the CDHO bands used to achieve the fit (bottom box). The wings of all peaks outside the region are included in the fitted spectrum but for clarity are not shown in the bottom box.

Table 1
Observed and fitted bands in the imaginary molar polarizability spectrum of liquid fluorobenzene

Observed $\tilde{\nu}$[a]	Fitted band			Sum of C_j[c]	Assignment[d]
	$\tilde{\nu}_j$[b]	Γ_j[b]	C_j[c]		
3960.0 VW	*I*				$\nu_2 + \nu_{16}$ (3959)
	3942.7	44.3	200.53		$\nu_3 + \nu_{16}$ (3946)
3905.6 VW	3907.0	27.6	235.09		$\nu_{10} + \nu_{21}$ (3907)
3903.9 VW	*I*				WV
3901.6 VW	*I*				WV
3899.0 VW	*I*				WV
~3895 VW Sh	*I*				
3891.5 VW	3891.1	23.7	186.81		$\nu_1 + \nu_{10}$ (3891)
3888.8 VW	*I*				WV
3885.5 VW	*I*				
3882.9 VW	*I*				WV
3880.0 VW	*I*				WV
~3877 VW Sh	*I*				
3874.0 VW	3874.8	16.3	89.09		
3869.9 VW	3870.0	32.9	154.61		$\nu_2 + \nu_{10}$ (3869)
3867.2 VW	3866.5	11.9	83.79		
~3865 VW Sh	*I*				WV
~3862 VW Sh	*I*				WV
~3859 VW Sh	*I*				WV
3853.9 VW	*I*				WV
3851.5 VW	*I*				WV
3849.1 VW	*I*				WV
~3840 VW Sh	*I*				$\nu_{10} + \nu_{22}$ (3843), $\nu_1 + \nu_{17}$ (3840)
3837.6 VW	*I*				WV
3834.5 VW	*I*				WV
3831.4 VW	*I*				WV
3828.7 VW	3830.8	24.8	410.37		
~3821 VW Sh	*I*				
~3819 VW Sh	*I*				$\nu_2 + \nu_{17}$ (3817)
3764.0 VW Br	3764.4	54.9	155.40		
3712.1 VW	3711.8	18.8	301.77		$\nu_{21} + \nu_{29}$ (3714)
3709.4 VW	*I*				WV
3683.8 VW	3683.3	25.2	228.23		
3660.2 VW	3660.3	9.3	86.72		$\nu_3 + \nu_{29}$ (3663)
3647.5 VW	3648.0	14.7	47.03		$\nu_{22} + \nu_{29}$ (3650)
3635.0 VW	3634.8	14.5	132.23		
3602.3 VW	3603.2	24.7	214.37		$\nu_1 + \nu_{11}$ (3604)
~3592 VW Sh	3588.1	17.6	95.92		$\nu_1 + \nu_{19}$ (3585)
3551.3 VW Br	3548.2	60.9	200.96		$\nu_{11} + \nu_{22}$ (3556), $\nu_3 + \nu_{19}$ (3549)
3477.3 VW	3477.4	20.1	59.06		
3375.4 VW	3377.0	7.5	7.05		
3193.6 VW	3190.6	51.7	841.09		$\nu_4 + \nu_{23}$ (3197), $2\nu_4$ (3191)
3151.6 VW	*I*				
3100.1 W	3101.5	12.3	1266.34		ν_{21} (CH Stretch)
3085.7 W	3086.2	9.4	1787.11		ν_1 (CH Stretch)
	3079.0	82.6	7352.03	12015	
~3072 W Sh	3073.5	16.2	2875.83		
3069.3 VW	*I*				
3063.0 W	3062.8	11.7	2905.00		ν_2 (CH Stretch)
3050.0 M	3049.7	8.8	3416.58		ν_3 (CH Stretch)
3037.0 W	3036.5	11.8	2037.04		ν_{22} (CH Stretch)
~3028 VW Sh	3027.1	28.3	1874.12		
2948.8 VW	2948.6	8.1	112.35		$\nu_5 + \nu_{24}$ (2953)
2935.1 VW Br	*I*				
2910.1 VW	2911.8	55.5	391.89		$2\nu_{24}$ (2915)
2889.4 VW	2888.3	9.1	90.23		
~2885 VW Sh	*I*				
2875.5 VW	2874.7	12.4	210.30		
~2853 VW Sh	*I*				
2816.0 VW	*I*				$\nu_2 - \nu_{20}$ (2821), $\nu_6 + \nu_{23}$ (2821), $\nu_5 + \nu_{25}$ (2820)
2791.3 VW	2789.2	21.6	104.83		$\nu_5 + \nu_{26}$ (2796)
2778.3 VW	2777.9	8.6	39.64		$\nu_{24} + \nu_{25}$ (2782)

Table 1 (*Continued*)

Observed $\tilde{\nu}$[a]	Fitted band			Sum of C_j[c]	Assignment[d]
	$\tilde{\nu}_j$[b]	Γ_j[b]	C_j[c]		
~2775 VW Sh	2771.6	23.7	15.24		
~2746 VW Sh	2744.6	16.2	163.57		$\nu_4 + \nu_7$ (2751), $\nu_4 + \nu_{27}$ (2751)
2742.2 VW	2741.2	3.6	5.80		
2709.5 VW	2710.2	17.1	92.19		$\nu_5 + \nu_6$ (2715)
~2697 VW Sh	2695.8	20.2	29.87		
~2656 VW Sh	2656.8	9.1	41.89		$\nu_4 + \nu_{28}$ (2662)
2647.0 VW	2647.0	9.4	133.19		$\nu_5 + \nu_7$ (2650), $\nu_5 + \nu_{27}$ (2650), $2\nu_{25}$ (2649)
~2628 VW Sh	2629.4	21.0	120.76		$\nu_{25} + \nu_{26}$ (2625)
~2618 VW Sh	2618.3	8.7	49.69		$\nu_8 + \nu_{23}$ (2622), $\nu_4 + \nu_8$ (2616), $\nu_7 + \nu_{24}$ (2613)
2611.8 VW	2611.7	9.1	302.35		$\nu_4 + \nu_8$ (2616), $\nu_7 + \nu_{24}$ (2613), $\nu_{24} + \nu_{27}$ (2613)
~2583 VW Sh	2584.1	7.2	45.86		
2577.6 VW	2577.3	11.3	299.33		$\nu_4 + \nu_{15}$ (2576)
~2572 VW Sh	2564.5	20.4	72.33		$\nu_5 + \nu_{28}$ (2561)
~2549 VW Sh	*I*				$\nu_6 + \nu_{25}$ (2545)
2543.4 VW	2542.4	25.5	144.70		
~2521 VW Sh	*I*				$\nu_{24} + \nu_{28}$ (2524), $\nu_6 + \nu_{26}$ (2521)
2513.4 VW	2513.8	16.5	65.47		$\nu_5 + \nu_8$ (2516)
2503.0 VW	2503.1	10.6	25.44		
2482.4 VW	2485.2	19.1	131.25		$\nu_5 + \nu_9$ (2490), $\nu_7 + \nu_{25}$ (2480), $\nu_{25} + \nu_{27}$ (2480)
~2462 VW Sh	2463.5	19.9	99.97		
~2453 VW Sh	2453.6	12.5	164.96		$\nu_7 + \nu_{26}$ (2456), $\nu_{26} + \nu_{27}$ (2456), $\nu_9 + \nu_{24}$ (2453)
2442.0 W	2443.4	12.4	385.53		$2\nu_6$ (2440)
~2436 W Sh	2437.4	7.8	58.19		
2432.9 W	2432.0	14.4	397.60		
2423.4 W	2424.5	15.2	312.56		$\nu_{13} + \nu_{23}$ (2419)
2399.1 W	2398.8	16.4	812.12		$\nu_4 + \nu_{10}$ (2401)
2372.0 VW	2374.4	18.4	326.90		$\nu_6 + \nu_7$ (2375), $\nu_6 + \nu_{27}$ (2375)
2371.7 VW	2366.3	8.7	73.28		$\nu_6 + \nu_7$ (2375), $\nu_6 + \nu_{27}$ (2375), $\nu_{26} + \nu_{28}$ (2367)
2347.7 VW	2346.9	16.8	194.62		$\nu_4 + \nu_{17}$ (2350), $\nu_8 + \nu_{25}$ (2345)
2319.8 M	2320.9	13.8	249.36		$\nu_8 + \nu_{26}$ (2321), $\nu_9 + \nu_{25}$ (2320)
2311.0 W	2311.0	8.7	457.16		$2\nu_7$ (2310), $2\nu_{27}$ (2310), $\nu_7 + \nu_{27}$ (2310)
2299.1 W	2298.9	10.9	419.13		$\nu_5 + \nu_{10}$ (2301), $\nu_9 + \nu_{26}$ (2296)
~2283 VW Sh	2282.8	22.3	209.28		$\nu_6 + \nu_{28}$ (2286), $\nu_4 + \nu_{18}$ (2281), $\nu_{12} + \nu_{25}$ (2280)
2258.4 VW	2258.5	16.9	149.26		$\nu_{10} + \nu_{24}$ (2263), $\nu_{12} + \nu_{26}$ (2256)
~2247 VW Sh	2242.2	28.0	126.66		$\nu_5 + \nu_{17}$ (2249), $\nu_6 + \nu_8$ (2241)
2220.8 W	2221.1	7.7	187.54		$\nu_{27} + \nu_{28}$ (2221), $\nu_7 + \nu_{28}$ (2221)
~2211 VW Sh	2216.9	13.0	104.20		$\nu_6 + \nu_9$ (2215), $\nu_4 + \nu_{29}$ (2209)
2199.9 VW	2202.3	32.7	187.70		$\nu_6 + \nu_{15}$ (2200)
2174.2 VW	2174.2	9.9	143.77		$\nu_7 + \nu_8$ (2176), $\nu_8 + \nu_{27}$ (2176)
~2163 VW Sh	2157.6	25.4	89.33		
~2151 VW Sh	*I*				$\nu_7 + \nu_9$ (2150), $\nu_9 + \nu_{27}$ (2150)
2130.1 VW	2130.7	14.5	66.47		$\nu_7 + \nu_{15}$ (2135), $2\nu_{28}$ (2132), $\nu_{10} + \nu_{25}$ (2130)
2111.9 VW	2110.8	17.7	100.58		$\nu_6 + \nu_{16}$ (2116), $\nu_4 + \nu_{11}$ (2114), $\nu_{12} + \nu_{27}$ (2110), $\nu_{10} + \nu_{26}$ (2106)
2084.8 VW	2084.9	10.4	52.97		$\nu_8 + \nu_{28}$ (2086)
2069.5 VW	2069.8	4.5	28.02		$\nu_{24} + \nu_{29}$ (2071)
~2033 W Sh	2035.2	17.1	450.90		
2020.2 W	2019.9	18.2	1495.12		$\nu_{12} + \nu_{28}$ (2021), $\nu_8 + \nu_9$ (2016)
1985.3 VW	1985.7	4.6	22.89		$2\nu_9$ (1990)
1959.6 W	1959.4	12.3	1235.71		$\nu_7 + \nu_{10}$ (1961), $\nu_{10} + \nu_{27}$ (1961), $2\nu_{15}$ (1960)
1936.9 W	1936.7	17.1	2826.00		$\nu_{25} + \nu_{29}$ (1937), $\nu_{12} + \nu_{15}$ (1935)
~1916 W Sh	1913.7	2.8	14.16		$\nu_8 + \nu_{16}$ (1916), $\nu_{26} + \nu_{29}$ (1914), $2\nu_{12}$ (1910)
1900.1 VW	*I*				$\nu_6 + \nu_{18}$ (1905), $\nu_5 + \nu_{30}$ (1899)
1872.9 W	1874.2	13.0	585.38		$\nu_{15} + \nu_{16}$ (1876), $\nu_{10} + \nu_{28}$ (1872)
1853.0 W	1852.8	15.7	2338.66		$\nu_{14} + \nu_{24}$ (1858), $\nu_{12} + \nu_{16}$ (1851)
~1834 W Sh	1832.8	5.8	30.19		$\nu_4 + \nu_{20}$ (1838), $\nu_6 + \nu_{29}$ (1833)
1826.3 W	1826.3	3.4	20.62		$\nu_8 + \nu_{10}$ (1826)
~1799 W Sh	1797.1	17.8	232.52		$\nu_9 + \nu_{10}$ (1801), $\nu_{13} + \nu_{15}$ (1798)
1775.5 W	1775.4	17.0	1540.44		$\nu_8 + \nu_{17}$ (1775), $\nu_{12} + \nu_{13}$ (1773)
~1733 W Sh	1734.0	8.0	220.85		$\nu_6 + \nu_{11}$ (1739), $\nu_5 + \nu_{20}$ (1737), $\nu_{15} + \nu_{17}$ (1734)
1713.7 W	1713.5	18.5	2665.74		$\nu_{13} + \nu_{16}$ (1714), $\nu_{12} + \nu_{17}$ (1709)
1694.1 W	1693.5	5.0	149.24		
1673.8 W	*I*				$\nu_{28} + \nu_{29}$ (1679), $\nu_7 + \nu_{11}$ (1674), $\nu_{11} + \nu_{27}$ (1674)
~1604 M Sh	1604.8	26.0	4680.06	6789	$\nu_9 + \nu_{29}$ (1608)
1601.4 S	1601.8	3.6	2198.94		ν_{23} (Ring Deformation)

Table 1 (*Continued*)

Observed $\tilde{\nu}$[a]	Fitted band			Sum of C_j[c]	Assignment[d]
	$\tilde{\nu}_j$[b]	Γ_j[b]	C_j[c]		
1595.7 S	1595.6	7.4	44766.60		ν_4 (Ring Deformation)
~1584 W Sh	1581.4	12.8	3475.94		$\nu_{11} + \nu_{28}$ (1584), $\nu_{16} + \nu_{18}$ (1581)
1525.8 M	1526.2	7.0	1669.82		
~1508 M Sh	1510.2	9.7	2138.37		$\nu_9 + \nu_{11}$ (1514), $2\nu_{17}$ (1509), $\nu_{13} + \nu_{18}$ (1503)
1494.8 S	1494.8	5.9	50207.68		ν_5 (HCC Deformation), $\nu_9 + \nu_{19}$ (1494)
~1489 S Sh	1490.1	10.4	11363.96		$\nu_{10} + \nu_{18}$ (1491)
1479.1 M	1478.8	10.2	9456.38		$\nu_{15} + \nu_{19}$ (1479)
~1475 W Sh	1474.5	8.1	2427.34		$\nu_{28} + \nu_{30}$ (1470)
1457.7 M	1457.7	3.0	2382.00	3300	ν_{24} (Ring and HCC Deformation)
	1453.7	7.0	918.10		$\nu_{12} + \nu_{19}$ (1454)
1394.3 W	1394.1	8.9	907.47		$\nu_7 + \nu_{20}$ (1397), $\nu_{16} + \nu_{19}$ (1394)
1329.2 W	*I*				
1324.6 W	1325.9	10.3	1538.42		ν_{25} (Ring and HCC Deformation), $\nu_{10} + \nu_{11}$ (1324)
1300.7 W	1300.5	5.7	315.87		ν_{26} (HCC bend)
1288.3 W	*I*				
~1255 M Sh	1254.8	12.5	1663.99		$\nu_{17} + \nu_{19}$ (1253), $\nu_5 - \nu_{20}$ (1253)
~1236 S Sh	1236.4	11.0	11960.86		$\nu_9 + \nu_{20}$ (1237)
~1231 S Sh	1231.7	11.5	9889.83		
~1224 S Sh	1224.6	10.2	22334.37	60957	$2\nu_{29}$ (1226), $\nu_{13} + \nu_{30}$ (1222), $\nu_{15} + \nu_{20}$ (1222)
1219.9 S	1220.6	9.0	22034.03		ν_6 (HCC Deformation)
	1217.0	7.9	16589.02		$\nu_{13} + \nu_{14}$ (1218)
	1213.4	8.2	7293.38		$\nu_{10} + \nu_{30}$ (1210)
	1196.7	3.7	137.05		$\nu_{12} + \nu_{20}$ (1197)
1187.2 M	1185.4	7.5	427.78		$\nu_{18} + \nu_{19}$ (1184)
1155.0 S	1155.0	5.0	10783.16		ν_7 (HCC Deformation), ν_{27} (HCC Deformation)
~1153 M Sh	1152.9	9.3	2879.96		$\nu_{14} + \nu_{17}$ (1154)
~1137 M Sh	1136.5	14.9	1463.69		$\nu_{16} + \nu_{20}$ (1138)
1103.3 W	1102.8	7.2	279.25		
1065.8 M	1066.0	4.3	4500.72		ν_{28} (HCC Deformation)
	1064.0	3.2	124.55		
~1062 M Sh	1062.9	8.2	2744.67		$\nu_{13} + \nu_{20}$ (1060)
1020.5 M	1020.7	3.8	2164.70		ν_8 (Ring and HCC Deformation)
~1017 M Sh	1017.8	8.1	1665.99		$\nu_{11} + \nu_{19}$ (1017), $\nu_{29} + \nu_{30}$ (1017), $\nu_{14} + \nu_{29}$ (1013)
~1007 W Sh	1007.2	9.3	277.47		
995.2 M	995.1	12.0	1998.76		ν_9 (Ring Deformation), $2\nu_{19}$ (998), $\nu_{17} + \nu_{20}$ (996)
979.9 W	981.2	13.6	289.13		ν_{15} (HCCC oop bend)
~976 W Sh	976.7	14.8	575.45		$\nu_6 - \nu_{20}$ (978)
~960 W Sh	958.4	22.5	700.43		ν_{12}? (HCCC oop bend)
~926 W Sh	926.9	13.0	120.53		$\nu_{18} + \nu_{20}$ (927), $\nu_{11} + \nu_{30}$ (923)
~915 W Sh	914.6	5.8	108.52		$\nu_7 - \nu_{20}$ (913)
895.5 M	896.0	7.4	7127.55	9727	ν_{16} (HCCC oop bend), $\nu_{14} + \nu_{19}$ (899)
~891 M Sh	893.6	7.6	2599.42		
874.3 M	873.6	5.5	422.16		
830.1 M	830.6	7.8	2817.40		
~825 M Sh	824.3	9.4	917.52		
~810 S Sh	809.5	4.4	2230.78		$2\nu_{30}$ (808)
805.7 S	806.0	4.9	12027.08	24978	ν_{10} (Ring Deformation)
~805 S Sh	804.6	7.4	12950.56		$\nu_{14} + \nu_{30}$ (804), $2\nu_{14}$ (800)
~778 M Sh	777.8	10.7	1065.32		$\nu_8 - \nu_{20}$ (779)
~757 S Sh	758.0	7.9	23414.45	73342	$\nu_{11} + \nu_{20}$ (761)
754.3 S	755.6	5.3	15721.16		ν_{17} (HCCC oop bend)
	753.6	4.7	14945.17		$\nu_9 - \nu_{20}$ (753)
~752 S Sh	751.4	4.4	12083.40		
	749.0	4.2	4997.13		
~746 S Sh	746.2	5.2	2181.08		
685.0 S	686.5	4.4	6835.40	22002	ν_{18} (HCCC oop bend)
	684.9	3.4	10328.49		
	682.9	4.7	4837.74		
651.5 M	651.5	7.6	551.47		$\nu_{16} - \nu_{20}$ (654)
~645 W Sh	645.3	3.8	27.35		$\nu_{14} + \nu_{20}$ (642)
612.7 W	613.0	3.4	119.63		ν_{29} (Ring Deformation)
~521 M Sh	521.7	4.0	670.10	5758	
518.5 S	519.4	3.5	1882.05		
	518.0	3.5	3205.38		ν_{11} (CF Stretch)

Table 1 (*Continued*)

Observed $\tilde{\nu}$[a]	Fitted band			Sum of C_j[c]	Assignment[d]
	$\tilde{\nu}_j$[b]	Γ_j[b]	C_j[c]		
~515 M Sh	515.7	4.4	356.54		$\nu_{17} - \nu_{20}$ (512)
~508 W Sh	508.6	6.0	613.74		
498.9 S	499.0	4.8	9878.72	11698	ν_{19} (HCCC oop bend)
~495 S Sh	496.0	5.6	1819.64		
~490 M Sh	489.8	2.3	11.63		
~481 M Sh	480.1	7.0	177.42		$2\nu_{20}$ (484)
~475 W Sh	475.1	4.1	56.34		
447.7 W	447.8	8.3	68.14		
427.0 W	428.2	2.1	8.89		
421.7 W	422.0	5.1	55.72		
~417 W Sh	417.5	1.0	6.04		
~414 W Sh	414.7	3.0	40.48		
~412 M Sh	412.2	1.3	11.41		
~407 M Sh	408.4	6.1	215.10	3658	
404.2 S	404.3	4.1	3431.48		ν_{30} (FCC bend)

[a] The unit is cm^{-1}. S indicates strong; M, medium; W, weak; VW, very weak; Sh, shoulder; and Br, broad.
[b] The unit is cm^{-1}. *I* indicates the feature was ignored in the fit.
[c] The unit is cm mol^{-1}. Divide by 1×10^5 to convert to the usual unit of km mol^{-1}.
[d] Herzberg's notation is used to label the vibrations. The assignments are limited to fundamentals, first overtones and active binary combinations (sum and difference). WV indicates the band is assigned to water vapour in the spectrometer. Descriptions of the vibrations are given for the fundamental vibrations. These motions were determined from the normal coordinates calculated [17] at the MP2 level of theory with the cc-pVDZ basis via Gaussian 03 [26].

box, visible differences occur at ~1650 cm^{-1}. In the bottom box, visible differences occur at ~1550, ~1350, ~1300, ~850, ~700, and 550 cm^{-1}.

In Fig. 2, the experimental and fitted spectra are shown in the top box while the peaks used to achieve the fit are shown in the bottom box. The only visible difference between the two is at ~1290 cm^{-1} where the fitted spectrum is below the experimental. Most of the peaks are visible in the experimental spectrum as peaks, shoulders, or changes of slope. It should be noted that the wings of all the peaks outside the region are included in the fitted spectrum, but for clarity these are not shown.

3. Results and discussion

3.1. Assignment of transitions

The vibrational representation for monohalobenzenes is $11A_1 + 3A_2 + 6B_1 + 10B_2$ under the point group C_{2v}, where by convention the *x*-axis is taken orthogonal to the plane of the molecule. Herzberg's notation [25] is used to number the vibrations throughout this paper. The A_2 vibrations are infrared inactive in the gas-phase while the others are infrared active. All first overtones and binary sum and difference bands except $A_1 \times A_2$ and $B_1 \times B_2$ are infrared active.

Included in Table 1 are the assignments of most of the bands used to fit the spectrum. The assignments of the bands are limited to fundamentals, first overtones and active binary sum and difference bands because ternary and larger combinations allow too many possibilities. It is expected that the first overtones and binary sum and difference bands should be the most intense, but it is noted that other overtones and combinations are possible and it is an impossible task to assign them from the current experimental measurements. The fundamentals are those reported previously [17]. Included in Table 1 for the fundamentals are brief descriptions of the vibrations. These motions were determined from the normal coordinates calculated [17] at the MP2 level of theory with the cc-pVDZ basis via Gaussian 03 [26]. The assignments of the overtones and combinations are presented as most probable assignments, and when the experimental work is complete on the monosubstituted benzenes, some refinement of these assignments may be possible.

In Table 1, in the "sum of C_j" column, the sums of the integrated intensities are reported for fundamentals that overlap with bands assigned to overtones or combinations. It is assumed that the total intensities are due to the fundamentals. While, the overtones and combinations may have inherent intensities, these will generally be small and will be neglected. At this stage it is not possible to determine how much of the intensity comes from the fundamental and how much comes from the overtones or combinations. Another complication is the fact that ν_7 and ν_{27} are both assigned to the same band, thus making their intensities inseparable. The ν_{20} fundamental is below the cut-off of the current measurements and as such no intensity has been determined for this vibration. This laboratory has recently obtained funding to purchase an FTIR spectrometer capable of making measurements down to 50 cm^{-1}. Some of the first studies carried out on this spectrometer will be the low wavenumber measurements of fluorobenzene to determine the intensity of ν_{20}.

The integrated intensity C_j is related to the transition moment, $\mathbf{R}_j$, under the assumption that the hot bands of the fundamental all contribute to the fundamental, by [3,27–29]

$$C_j = \frac{N_A \pi}{3hc_0} g_j \tilde{\nu}_j |\boldsymbol{R}_j|^2, \quad (1)$$

where N_A is the Avogadro's number; h, the Planck's constant; c_0, the speed of light in a vacuum, and g_j, the degeneracy of the transition. The integrated intensity can also be related to the square of the dipole moment derivative with respect to the jth normal coordinate, $\mu_j^2 = |\partial\vec{\mu}/\partial Q_j|^2$, under the double harmonic approximation by [3]

$$C_j = \frac{N_A}{24\pi c_0^2} g_j \mu_j^2. \quad (2)$$

The transition moments and square of the dipole moment derivatives of the fundamentals of fluorobenzene are given in Tables 2 and 3, respectively, along with those previously reported for benzene-d_1 [9], bromobenzene-h_5 [11] and bromobenzene-d_5 [13]. The estimated [8] 10% uncertainty in C_j results in an approximately 5% uncertainty in the transition moments and dipole moment derivatives.

Under the double harmonic approximation, the integrated intensities of different isotopomers can be compared by the F-Sum rule [30,31]. In addition to the requirements of the double harmonic approximation, the F-Sum is only applicable if either the molecule does not have a permanent dipole moment or if the summation is over vibrations that belong to a symmetry species that does not involve a rotation of the permanent dipole of the molecule. The F-Sum, expressed in terms of the integrated intensity C_j and the vibrational wavenumber $\tilde{\nu}_j$, is

$$\sum \frac{C_j}{\tilde{\nu}_j^2} = \text{constant} \quad (3)$$

For fluorobenzene the dipole moment is 1.6 D in the gas phase [32], and thus, technically, the sum rules only apply to the A_1 vibrations (the only symmetry species that does not rotate the permanent dipole). However, as a first approximation we can compare the intensities using the sum rule.[1] The F-Sums are given in Table 4, along with the previous values for benzene-d_1 [9], bromobenzene-h_5 [11], bromobenzene-d_5 [13], benzene-h_6 [7] and benzene-d_6 [8]. Remarkably, the F-Sums for the out-of-

Table 2
Transition moments for fundamental vibrations of monosubstituted benzenes

Vibration	Symmetry	$\|\boldsymbol{R}_j\|$ (D)			
		C_6H_5F	C_6H_5D [9]	C_6H_5Br [11]	C_6D_5Br [13]
ν_1	A_1	0.0350	0.0344	0.0217	0.00791
ν_2	A_1	0.0173	0	0.0190	0.0118
ν_3	A_1	0.0188	0.0149	0.00744	0.0168
ν_4	A_1	0.0940	0.0266	0.0366	0.0254
ν_5	A_1	0.103	0.0116	0.0718	0.0849
ν_6	A_1	0.125	0.0439	0.0179	0.0921
ν_7	A_1	0.0542[a]	0.0158	0.0584	0.0358
ν_8	A_1	0.0258	0.0431	0.0590	0.0183
ν_9	A_1	0.0252	0.0131	0.0387	0.0391
ν_{10}	A_1	0.0988	0.0133	0.0653	0.0807
ν_{11}	A_1	0.0591	0	0.0247	0
ν_{12}	A_2	0	0	0.0291	0
ν_{13}	A_2	0	0	0.0166	0
ν_{14}	A_2	0	0	0	0
ν_{15}	B_1	0.0096	0.0140	0.0296	0.00366
ν_{16}	B_1	0.0585	0.0304	0.0350	0.0262
ν_{17}	B_1	0.175	0.0983	0.171	0.0507
ν_{18}	B_1	0.101	0.0896	0.0966	0.146
ν_{19}	B_1	0.0859	0.176	0.0812	0.108
ν_{20}	B_1	0	0	0.0381	0
ν_{21}	B_2	0.0113	0.0356	0.0277	0.0151
ν_{22}	B_2	0.0145	0.0121	0.00837	0.0210
ν_{23}	B_2	0.0368	0.0103	0.0342	0.0580
ν_{24}	B_2	0.0267	0.0445	0.0496	0.0374
ν_{25}	B_2	0.0191	0.0061	0.0192	0.0178
ν_{26}	B_2	0.0087	0.0080	0.0179	0.0510
ν_{27}	B_2	0.0542[a]	0.0194	0.0189	0.0207
ν_{28}	B_2	0.0365	0.0295	0.0537	0.00366
ν_{29}	B_2	0.0078	0.0387	0.0134	0.0183
ν_{30}	B_2	0.0534	0	0.00477	0

[a] ν_7 and ν_{27} are both assigned to 1155 cm^{-1}, making it impossible to separate the integrated intensity and determine the individual transition moments. The value given is the maximum transition moment. The actual transition moment will between 0 and 0.0542 D.

Table 3
Dipole moment derivatives for fundamental vibrations of monosubstituted benzenes

Vibration	Symmetry	μ_j^2 ($D^2 Å^{-2} u^{-1}$)			
		C_6H_5F	C_6H_5D [9]	C_6H_5Br [11]	C_6D_5Br [13]
ν_1	A_1	0.225	0.215	0.0854	0.00856
ν_2	A_1	0.054	0	0.0652	0.0188
ν_3	A_1	0.064	0.039	0.0100	0.0381
ν_4	A_1	0.837	0.095	0.2421	0.0596
ν_5	A_1	0.938	0.013	0.482	0.574
ν_6	A_1	1.14	0.168	0.0281	0.510
ν_7	A_1	0.201[a]	0.018	0.238	0.0728
ν_8	A_1	0.040	0.114	0.221	0.0171
ν_9	A_1	0.037	0.010	0.0906	0.0739
ν_{10}	A_1	0.467	0.010	0.253	0.248
ν_{11}	A_1	0.108	0	0.0243	0
ν_{12}	A_2	0	0	0.0157	0
ν_{13}	A_2	0	0	0.0158	0
ν_{14}	A_2	0	0	0	0
ν_{15}	B_1	0.005	0.011	0.0514	0.000654
ν_{16}	B_1	0.182	0.050	0.0656	0.0302
ν_{17}	B_1	1.37	0.448	1.28	0.0937
ν_{18}	B_1	0.411	0.336	0.379	0.691
ν_{19}	B_1	0.219	1.12	0.179	0.282
ν_{20}	B_1	0.000	0	0.0159	0
ν_{21}	B_2	0.024	0.232	0.140	0.0309
ν_{22}	B_2	0.038	0.026	0.0126	0.0594
ν_{23}	B_2	0.129	0.010	0.109	0.307
ν_{24}	B_2	0.062	0.170	0.211	0.109
ν_{25}	B_2	0.029	0.003	0.0288	0.0241
ν_{26}	B_2	0.006	0.005	0.0240	0.158
ν_{27}	B_2	0.201[a]	0.026	0.0245	0.0213
ν_{28}	B_2	0.084	0.056	0.183	0.000654
ν_{29}	B_2	0.002	0.077	0.00656	0.0116
ν_{30}	B_2	0.068	0	0.000333	0

[a] ν_7 and ν_{27} are both assigned to 1155 cm^{-1}, making it impossible to separate the integrated intensity and determine the individual dipole moment derivatives. The value given is the maximum dipole moment derivative. The actual square of the dipole moment derivative will between 0 and 0.201 D^2 $Å^{-2}$ u^{-1}.

[1] A nonzero dipole moment necessitates the inclusion of the rotational motion as well as knowledge of the force constants [25]. At this time, the force constants are not known and this is the only option available. After the liquid force field is determined as described in the summary, further refinement of this may be possible.

Table 4
F-Sums for fundamental vibrations of monosubstituted benzenes

Symmetry	$\sum \frac{C_j}{\tilde{\nu}_j^2}$ (cm^3 mol^{-1})					
	C_6H_5F	C_6H_5D [9]	C_6H_5Br [11]	C_6D_5Br [13]	C_6H_6 [7]	C_6D_6 [8]
A_1	0.147–0.155[a]	0.014	0.090	0.089		
B_2	0.032–0.040[a]	0.015	0.021	0.024		
$A_1 + B_2$[b]	0.187	0.030	0.111	0.113	0.030	0.031
B_1[c]	0.235	0.242	0.248	0.233	0.279	0.252
Total	0.422	0.272	0.361	0.346	0.309	0.283

[a] ν_7 and ν_{27} are both assigned to 1155 cm^{-1}, making it impossible to separate the integrated intensity. The ranges given are for when the intensity is assigned completely to one vibration. The actual value will be somewhere in between but is impossible to determine from the current measurements.
[b] For C_6H_6 and C_6D_6, the values listed are for the E_{1u} vibrations.
[c] For C_6H_6 and C_6D_6, the values listed are for the A_u vibrations.

plane B_1 vibrations are the same within experimental error. The only value that is significantly different is that for benzene-h_6. As was pointed out previously [9], this is most likely due to the fact that the A_{2u} fundamental of benzene is so strong and very difficult to measure experimentally. Thus, one possibility is to conclude that the dipole moment derivatives of the out-of-plane vibrations are not affected by the halogen substitution. The usual assumption is that the electron withdrawing nature of the halogen substitutent and the differing intermolecular interactions should affect the vibrational intensities. However, this may not be case for the out-of-plane vibrations. This is in agreement with what was determined from the comparison [21,33] of the benzene intensities in the liquid- and gas-phases. However, at this stage it is impossible to make a firm conclusion and it could be just a coincidence that multiple differences in the vibrations between the different molecules offset each other and the F-Sum total remains relatively constant. It is encouraging and worth further exploration. This will be pursued by attempting a complete force field analysis for the different molecules and eventually by comparing the dipole moment derivatives with respect to internal coordinates as was done for benzene [21,33].

The in-plane fundamentals are enhanced by the halogen substitution, with the fluorobenzene in-plane vibrations being about six times as strong as the benzene vibrations. The bromobenzene vibrations are about four times as strong. Since both ν_7 and ν_{27} are in-plane vibrations, the inseparability of their intensities discussed above does not affect the overall intensity of the in-plane vibrations. Since the in-plane F-Sums are variable, it is necessary to determine the dipole moment derivatives with respect to internal coordinates to further explore the effect of the halogen substitution. This will be explored in a future paper in this series.

The next stage of this work is to try and resolve the intensities of ν_7 and ν_{27}. To this end, ab initio calculations will be attempted to try and help partition the intensities of these two vibrations. In addition, the force field analysis of fluorobenzene and the two bromobenzene isotopomers previously published [11,13] will be carried out to transform the dipole moment derivatives with respect to normal coordinates to dipole moment derivatives with respect to internal coordinates. This will enable the comparison of the dipole moment derivatives for the different benzene compounds and provide insight into how the intermolecular interactions in these liquids affect the charge distribution of the benzene ring and how this in turn affects the vibrational intensities.

4. Summary

The first detailed vibrational assignment of liquid fluorobenzene is reported. The imaginary molar polarizability spectrum, $a''_m(\tilde{\nu})$, was fitted with 169 CDHO bands and the integrated intensity, C_j, calculated analytically from the fitted parameters for each band. The integrated intensities were determined for the fundamentals with the exception of ν_{20}. This vibration will be examined in the near future and reported in a future paper that completes the analysis of fluorobenzene. The intensities of ν_7 and ν_{27} could not be separated and had to be treated together.

By comparing the intensities of the fluorobenzene vibrations with those of three isotopomers of benzene and two isotopomers of bromobenzene, it was determined that the integrated intensities of the out-of-plane fundamentals are not affected electronically by the halogen substitution but only by a mass effect. Thus, for the purposes of the out-of-plane fundamentals, the halosubstituted benzenes can be treated as isotopomers of benzene. However, for the in-plane vibrations the intensities are affected both electronically and mechanically. This is consistent with the earlier conclusions from the comparison of the gaseous and liquid intensities of benzene where it was determined that the out-of-plane vibrations were constant between the two phases while the in-plane vibrations varied by as much as a factor of two.

In a future paper, the force field analysis of fluorobenzene and bromobenzene will be used to transform the dipole moment derivatives from normal coordinates to internal coordinates. This will allow the comparison of the dipole moment derivatives to be further refined between the different benzene compounds.

Acknowledgements

C.D.K. thanks the Natural Sciences and Engineering Research Council of Canada and the Office of Research and

Academic Institutes, Cape Breton University for research grants in support of this work.

References

[1] E.B. Wilson Jr., Phys. Rev. 45 (1934) 706.
[2] J.E. Bertie, S.L. Zhang, C.D. Keefe, Vib. Spectrosc. 8 (1995) 215.
[3] J.E. Bertie, S.L. Zhang, C.D. Keefe, J. Mol. Struct. 324 (1994) 157.
[4] C.D. Keefe, J. Mol. Spectrosc. 205 (2001) 261.
[5] J.E. Bertie, C.D. Keefe, R.N. Jones, Can. J. Chem. 69 (1991) 1609.
[6] J.E. Bertie, R.N. Jones, C.D. Keefe, Appl. Spectrosc. 47 (1993) 891.
[7] J.E. Bertie, C.D. Keefe, J. Mol. Struct. 695/696 (2004) 39.
[8] J.E. Bertie, C.D. Keefe, Fresenius J. Anal. Chem. 362 (1998) 91.
[9] J.E. Bertie, Y. Apelblat, C.D. Keefe, J. Mol. Struct. 550/551 (2000) 135.
[10] C.D. Keefe, J. Pittman, Appl. Spectrosc. 52 (1998) 1062.
[11] C.D. Keefe, L.A. Donovan, S.D. Fleet, J. Phys. Chem. A. 103 (1999) 6420.
[12] C.D. Keefe, L.A. Donovan, J. Mol. Struct. 597 (2001) 259.
[13] C.D. Keefe, J.K. Pearson, J. Mol. Struct. 751 (2005) 190.
[14] C.D. Keefe, S. MacInnis, T. Burchell, J. Mol. Struct. 610 (2002) 253.
[15] C.D. Keefe, S. MacInnis, J. Mol. Struct., submitted for publication.
[16] C.D. Keefe, E. Brand, J. Mol. Struct. 691 (2004) 181.
[17] C.D. Keefe, J. Barrett, L.L. Jessome, J. Mol. Struct. 734 (2005) 67.
[18] J.E. Bertie, R.N. Jones, Y. Apelblat, C.D. Keefe, Appl. Spectrosc. 48 (1994) 127.
[19] C.D. Keefe, J.K. Pearson, A. MacDonald, J. Mol. Struct. 655 (2003) 69.
[20] C.D. Keefe, J.E. Bertie, Spectrochim. Acta Part A, submitted for publication.
[21] C.D. Keefe, J.E. Bertie. Spectrochim. Acta Part A, submitted for publication.
[22] C.D. Keefe, Chem. Phys., submitted for publication.
[23] C.D. Keefe, J. Mol. Struct. 641 (2002) 165.
[24] J. McClave, F. Dietrich, T. Sincich, Statistics, seventh ed., Prentice-Hall, Upper Saddle River, 1997, pp. 553–554.
[25] G. Herzberg, Molecular Spectra and Molecular Structure. II. Infrared and Raman Spectra of Polyatomic Molecules, D. Van Nostrand Company, Princeton, 1945.
[26] M.J. Frisch, G.W. Trucks, H.B. Schlegel, G.E. Scuseria, M.A. Robb, J.R. Cheeseman, J.A. Montgomery, Jr., T. Vreven, K.N. Kudin, J.C. Burant, J.M. Millam, S.S. Iyengar, J. Tomasi, V. Barone, B. Mennucci, M. Cossi, G. Scalmani, N. Rega, G.A. Petersson, H. Nakatsuji, M. Hada, M. Ehara, K. Toyota, R. Fukuda, J. Hasegawa, M. Ishida, T. Nakajima, Y. Honda, O. Kitao, H. Nakai, M. Klene, X. Li, J.E. Knox, H.P. Hratchian, J.B. Cross, C. Adamo, J. Jaramillo, R. Gomperts, R.E. Stratmann, O. Yazyev, A.J. Austin, R. Cammi, C. Pomelli, J.W. Ochterski, P.Y. Ayala, K. Morokuma, G.A. Voth, P. Salvador, J.J. Dannenberg, V.G. Zakrzewski, S. Dapprich, A.D. Daniels, M.C. Strain, O. Farkas, D.K. Malick, A.D. Rabuck, K. Raghavachari, J.B. Foresman, J.V. Ortiz, Q. Cui, A.G. Baboul, S. Clifford, J. Cioslowski, B.B. Stefanov, G. Liu, A. Liashenko, P. Piskorz, I. Komaromi, R.L. Martin, D.J. Fox, T. Keith, M.A. Al-Laham, C.Y. Peng, A. Nanayakkara, M. Challacombe, P.M.W. Gill, B. Johnson, W. Chen, M.W. Wong, C. Gonzalez, J.A. Pople, Gaussian 03, Revision B.05, Gaussian, Inc., Pittsburgh, PA, 2003.
[27] J. Fahrenfort, in: M. Davies (Ed.), Infra-Red Spectroscopy and Molecular Structure: An Outline of the Principles, Elsevier, 1963.
[28] J.W. Warner, M. Wolfsberg, J. Chem. Phys. 78 (1983) 1722.
[29] M.J. Dignam, Appl. Spectrosc. Rev. 21 (1988) 99.
[30] B. Crawford Jr., J. Chem. Phys. 20 (1952) 977.
[31] J.C. Decius, J. Chem. Phys. 20 (1952) 1039.
[32] D.R. Lide (Ed.), CRC Handbook of Chemistry and Physics (Electronic Version), 79th ed., Chemical Rubber Company, 1999.
[33] J.E. Bertie, C.D. Keefe, J. Chem. Phys. 101 (1994) 4610.